

Centrifugal effects in $N\Delta$ states

J.A. Niskanen

*Helsinki Institute of Physics, PO Box 64,
FIN-00014 University of Helsinki, Finland **

(Dated: April 23, 2020)

Abstract

Recently it has been pointed out that in the two-baryon $N\Delta$ or $\Delta\Delta$ system the width of the state is greatly diminished due to the relative kinetic energy of the two baryons, since the internal energy of the particles, available for pionic decay, is smaller. For nonzero orbital angular momenta this effect becomes state dependent. Also the real part of the $N\Delta$ energy can get contribution from the centrifugal barrier leading to rotational series of diffuse states. Obviously, these states may have an interpretation as isospin one dibaryons. Direct and explicit calculations for this are presented with some details of the coupled state wave functions displayed. With finite expectation values of these repulsive effects it may be possible to define state dependent effective thresholds for $N\Delta$ states and these, in turn, can show resonant like behavior.

PACS numbers: 25.80.-e, 21.85.+d, 13.75.-n, 24.10.Ht

Keywords: dibaryons, resonances

* jouni.niskanen@helsinki.fi

I. INTRODUCTION

The role of the $\Delta(1232)$ resonance has a long and established history in the pion-nucleon interaction and also in the NN interaction and plays a outstanding part in their inelasticities [1, 2]. Pionic inelasticities would be even idiomatic for probing intermediate $N\Delta$ components arising from incident NN states above the πNN threshold. Isovector meson, pion, exchange (and also ρ exchange) can excite an $N\Delta$ state, which in turn decays. The process is inseparable from elastic NN scattering and their strong interaction.

As the simplest such reaction, $pp \rightarrow d\pi^+$ was intensely studied in the late 70's and 80's at "meson factories" SIN, LAMPF and TRIUMF. For a modern review see e.g. Ref. [3]. Experiments indicate univocally the Δ peaking in the total cross section at about 580 MeV laboratory energy [4, 5], which, along with the differential cross section and transverse analyzing power, were also reasonably predicted by a coupled channel $N\Delta$ calculation without virtually any free parameters [6]¹. Further, spin correlations and deuteron polarization were given predictions [7, 8], which were promptly confirmed [9, 10]. The success of the calculations was mainly due to two $N\Delta$ admixtures generated from the initial nucleons: $^1D_2(NN) \rightarrow ^5S_2(N\Delta)$ and $^3F_3(NN) \rightarrow ^5P_3(N\Delta)$ sometimes dubbed as "dibaryons"². The latter was probably the first appearance of such a high partial wave appearing as important [6]. It may be noted that the coupled channel $N\Delta$ agreement with experiment was actually better than a six-parameter dibaryon fit [11].

Later an improvement [12] was done, which decreased the widths of the $N\Delta$ states, so far normally considered as the free Δ width with just appropriate kinematic adjustment [13, 14]. Namely, there is relative kinetic energy in the $N\Delta$ intermediate state, whose role should be considered in more detail. Obviously this kinetic portion is not usable for the (internal) pionic decay of the Δ 's. The width in turn is used as a uniform imaginary potential in the coupled $N\Delta$ system. Further, because the $N\Delta$ wave function becomes now necessarily spatially constrained (must vanish asymptotically) both below and also above the $N\Delta$ threshold, this kinetic energy is not arbitrary. Its average is finite and can be calculated from the Fourier transform of the wave function. The resulting kinematic suppression of the width was taken into account in the calculations of Ref. [12] for $pp \rightarrow d\pi^+$, but explicit width

¹ A form factor to account for the nucleon and Δ size could be considered as a free parameter, though it was taken from OBE potentials.

² A third essential ingredient was the axial charge and s -wave pion rescattering in the $^3P_1(NN)$ and associated $N\Delta$ waves.

results were only published recently [17]. Also rather strong sensitivity of the width was seen on the relative orbital angular momenta of the baryons. In addition to the improved agreement in the old reaction $pp \rightarrow d\pi^+$, the reduction of the width has great renewed relevance for interpretations of the $I(J^P) = 0(3^+)$ resonance recently discovered at the WASA@COSY detector of Forschungszentrum Jülich and labeled as $d'(2380)$ dibaryon [15, 16]. Its nominal mass 2380 MeV is 80 MeV below the $\Delta\Delta$ threshold and its width only 70 MeV, less than that of a free Δ . A calculation [17], similar to that shortly described above, gives just such a decreased value for the ${}^7S_3(\Delta\Delta)$ state coupled to ${}^3D_3(NN)$. A similar drastic suppression of the double Δ system width is also found by Gal and Garcilazo [18, 19] from coupled pion-baryon Faddeev calculations.

Further, in these reactions and NN scattering in different partial waves also the $N\Delta$ centrifugal barrier directly diminishes the wave functions. Although this suppression is expected to be naturally sensitive to $L_{N\Delta}$, also the orbital angular momentum of the initial nucleons may even favor transitions into $N\Delta$ in some sense. Namely, within the interaction range the reduction of the centrifugal barrier can compensate the $N\Delta$ mass difference in the excitation if $L_{N\Delta} < L_{NN}$, as seen in Ref. [20] as an explanation for $T = 1$ enhancements ($T = 1$ “dibaryons”). From the above considerations it is clear that just a single number cannot account for the effective two-baryon pole position in different partial waves.

Because the internal kinematics of the $N\Delta$ system has been seen to have a significant effect on its width, i.e. the imaginary part of the interaction [17], it is also of interest to see the effect on the real part of the energetics. Due to the confinement of the $N\Delta$ wave function, similar to bound systems in quantum mechanics, one might expect some kind of imitated quantization of the energy to appear - as noted above about the finite distribution of kinetic energy. In this kind of situation the angular momentum is directly related to the energy and this aspect of the kinetic energy is our central point now. Thus, if the expectation value of the centrifugal barrier $\hbar^2/2mr^2$ is well defined and reasonably constant over various $N\Delta$ configurations and NN energies one might expect also a reasonably well defined rotational series $\propto L_{N\Delta}(L_{N\Delta} + 1)$ to appear as effective channel thresholds. This is the direction to proceed now.

In fact, a very phenomenological calculation [20] gave some hints for this possibility. The work compared a phenomenological phase-fitted potential [21] and the same potential supplemented by an $N\Delta$ channel. To remove the double counting of attraction due to the

extra $N\Delta$ component, a repulsion $[V_2(r)]^2/\Delta E$ was added to mimic in a closure approximation the second order Δ effect. Here $V_2(r)$ is the $NN \leftrightarrow N\Delta$ transition potential and ΔE an average energy denominator adjusted for phase equivalence of the coupled and uncoupled calculations. It was seen that ΔE followed quite well such a rotational series with $\hbar^2/2mr^2 \approx 40$ MeV indicating about 1 fm as the effective channel radius. A remarkable thing was that this pattern actually corresponded well the series of isospin one dibaryons reported in Refs. [22, 23]. An additional criterion for a “dibaryon” to appear in the $N\Delta$ series was that $L_{N\Delta} < L_{NN}$, meaning that in the $NN \rightarrow N\Delta$ transition the orbital angular momentum decreases. For short range energetics this is a natural expectation, since then the $\Delta - N$ mass barrier is partly compensated by massive reduction of the centrifugal barrier favoring the tunneling into the $N\Delta$ channel.

The aim of this paper is to study in a simple transparent way some phenomenological aspects of how the relative kinetic energy between the two intermediate baryons influences the overall dynamics of the two-baryon system and, in particular, to calculate explicitly the expectation value of the centrifugal barrier for realistic coupled channel $N\Delta$ wave functions. First, in Sec. II a brief review is given about the formalism before proceeding to calculations and results in III.

II. FORMALISM

Pionic excitation of the $N\Delta$ (and $\Delta\Delta$) components into NN configurations was already suggested in an early paper by Sugawara and von Hippel [24]. The coupled channel formalism is generally described in the reviews [1, 2] and relevant details of the interactions are provided in Ref. [6]. Also essential updates and improvements are given in Ref. [12] mainly intended for the reaction $pp \rightarrow d\pi^+$, but extending relevantly in V_2 and in the width for more general $N\Delta$ dynamics. In particular, the peak of this reaction may be the best constraint on its dominant transition potential V_2 . The structure can be presented routinely by the coupled radial Schrödinger equation

$$\left[\frac{\hbar^2}{2m} \left(\frac{d^2}{dr^2} - \frac{L(L+1)}{r^2} \right) - V_1(r) + E \right] u(r) = V_2 w(r) \quad (1)$$

$$\left[\frac{\hbar^2}{2m'} \left(\frac{d^2}{dr^2} - \frac{L'(L'+1)}{r^2} \right) - V_3(r) + (E - \Delta) \right] w(r) = V_2 u(r) \quad (2)$$

for the NN and $N\Delta$ wave functions $u(r)$ and $w(r)$ respectively. Here the generic channel potentials are denoted by $V_i(r)$, and L (L') and m (m') present the angular momentum and reduced mass of the NN ($N\Delta$) system. The $\Delta - N$ mass difference $M_\Delta - M_N$ is abbreviated as Δ , with M_Δ taken as the position of the pole 1310 MeV rather than the nominal mass [25]. Above pion production threshold it is complemented by the state dependent width [17] into the form $\Delta - i\Gamma/2$. Thus, effectively the width acts as a constant imaginary part in the potential making the $N\Delta$ channel wave function $w(r)$ asymptotically vanishing. The asymptotically free radial NN wave function with momentum k can be presented and normalized with the descriptive form $u_{NN}(r) \sim kr \exp(i\delta_L) j_L(kr + \delta_L)$, where the phase shift may now be complex. For real interactions and below open channels it is common to the total wave function (with all channels). As a numerical comment, one should remember the rather slow asymptotic convergence of the regular and irregular Bessel function combination [26] $u_{NN}(r) \sim kr \exp(i\delta_L) [\cos \delta_L j_L(kr) - \sin \delta_L n_L(kr)]$ to this form for $L \neq 0$. The inclusion of more possible channels in the system (1) - (2) is obvious.

Also it is interesting to note the emergence of inelasticity above the $\Delta - N$ threshold even without any imaginary potential. With the opening of the $N\Delta$ channel unitarity in the NN sector is lost. Similar to the case with the tensor force, then the single parameter, the NN phase shift, is not sufficient any more to describe the asymptotics but a transition amplitude (analogous to ϵ_J) and scattering of the N and the Δ would be necessary. Below this threshold it is still possible to describe the scattering wave functions as real (by switching off the common overall phase $\exp(i\delta_L)$). In this case the still closed $N\Delta$ channel wave function $w(r)$ behaves asymptotically like $\exp(-\kappa r)$ with $\kappa = \sqrt{2m'(\Delta - E)}/\hbar$. Apparently at $N\Delta$ threshold the extension of the wave function becomes very large producing a cusp in the NN phase shift. Also the overlap integral of the amplitude in e.g. $pp \rightarrow d\pi^+$ would maximize grossly overestimating the cross section. Above threshold the phases (arguments) of both wave functions $u(r)$ and $w(r)$ depend on the channels and even on the radius r . In this case the $N\Delta$ wave function $w(r)$ behaves like an outgoing spherical wave $\propto \exp(ik'r)$ or more accurately $k'r h_L^+(k'r)$ with $k' = \sqrt{2m'(E - \Delta)}/\hbar$. The oscillatory behavior decreases overlap integrals from the cusp peak values. Probably in this case it would be possible to define scattering eigenfunctions and corresponding phase shifts like those of Blatt and Biedenharn [27]. However, in the presence of the constant imaginary potential $-i\Gamma/2$ this parametrization is not useful. In this case complexity appears already below the nominal

channel threshold adding to the damping and bringing in some oscillatory behaviour. Just at threshold the asymptotic suppression from the width should behave like $\sim \exp(-\gamma r)$ and include also corresponding oscillation with wave number $\gamma = \sqrt{m'\Gamma/(2\hbar^2)}$ (interfering with the effect of $V_2(r)u(r)$). The width moderates and rounds the cusp peak down. Above threshold this damping effect is sustained along with oscillations having the natural wave number k' given above.

Among the interactions the most important is the transition potential $V_2(r)$, based on one pion exchange supplemented with ρ exchange. Heavy meson exchanges to describe short-range interactions may not be favoured in present day effective field theories, but the main point is that this potential is thoroughly tested in the reaction $pp \rightarrow d\pi^+$ [12] and is now used only to imply the form of the associated $N\Delta$ component in detail. The diagonal $V_1(r)$ in the NN sector is taken as the old phenomenological Reid potential [21] modified to give the correct phase shifts in the presence of the $N\Delta$ excitation [6, 12, 28]. The $N\Delta$ potential $V_3(r)$ is not in our primary interest presently and is neglected. In NN scattering it would only appear hindered behind iterated V_2 . The width is calculated along the lines of Ref. [17], exhibited there for the most important and interesting states. In addition to the fact of giving rise to inelasticities and making also the NN wave function $u(r)$ complex, it causes also rather strong repulsion [29, 30] decreasing the attractive effect due to $N\Delta$ excitation. And it is state dependent as expressed in the Introduction.

To see the effect of the centrifugal barrier and the possible appearance of the rotational series one needs the straightforward expectation value

$$\langle \frac{1}{r^2} \rangle = \frac{\int_0^\infty |w(r)|^2 / r^2 dr}{\int_0^\infty |w(r)|^2 dr}. \quad (3)$$

Apparently this is simpler than the calculation [12, 17]

$$\Gamma_3 = \frac{2}{\pi} \frac{\int_0^{p_{\max}} |\Psi_{N\Delta}(p)|^2 \Gamma(q) p^2 dp}{\int_0^\infty |\Psi_{N\Delta}(r)|^2 r^2 dr} \quad (4)$$

for the width requiring the Fourier transform of the wave function and relevant restraints for the kinematically allowed momenta p and $q(p)$. The series $\langle \hbar^2/(2m'r^2) \rangle L'(L'+1)$ should be built on top of the mass difference Δ . In fact, one can also calculate the still missing kinetic energy $\langle -\hbar^2/2m' \partial^2/\partial r^2 \rangle$, associated with the radial degree of freedom, to be added to the nominal threshold Δ . Most naturally this can be calculated as the expectation value of $p^2/2m'$ in the momentum representation as in Eq. (4).

III. RESULTS

A. $N\Delta$ component magnitudes

In this section we study first details of the $N\Delta$ components connected to isospin one NN wave functions for various angular momentum configurations and then calculate consequent energy expectation values relevant as effective channel thresholds.

Figure 1 presents the radial dependence of the absolute values of the $N\Delta$ wave function components as described in the previous section. The uppermost functions present the ${}^5S_2(N\Delta)$ (solid curve), ${}^5D_2(N\Delta)$ (dashed) and ${}^5G_2(N\Delta)$ (dotted) states associated with the incident ${}^1D_2(NN)$ partial wave at three laboratory energies. This is the lowest lying “dibaryon” from NN phase shifts (apart from the deuteron and the sharp low-energy maximum in the quasibound NN 1S_0 wave). The position of the peak is practically independent of energy, for high energies at slightly smaller distance. Even up to 700 MeV the dominant S -wave maximum remains at about 1.1 – 1.2 fm, and the D - and G -wave variations from this distance are also negligible.³ Such weak energy dependence was also observed in Ref. [20] in the energy denominator ΔE of the second order effective repulsion $V_2^2/\Delta E$ to cancel the attraction due to the $N\Delta$ coupling and keep phase equivalence of pure single channel NN scattering and the coupled model. The repulsive influence of the centrifugal barrier is clear in the ordering of sizes, even more notably considering that the relative strengths of the (radially identical tensor type) transition potentials would be in opposite ordering 20 : (−23) : 31 for ${}^5S_2(N\Delta)$, ${}^5D_2(N\Delta)$ and ${}^5G_2(N\Delta)$, respectively [6]. However, in spite of this, the position of the maximum is remarkably independent of L' . The shoulders in r -dependence are due to either the real or imaginary part passing through zero. It might be reminded that the present 578 MeV result is related to the one in Fig. 1 of Ref. [17], where just the real part of the wave function was presented.

The second clear “dibaryon” candidate in NN scattering [22] and pion production [6] appears in the ${}^3F_3(NN)$ initial state shown in the second row of Fig. 1. Again the lowest $L' = L - 2$ coupled channel angular momentum 5P_3 (solid curve) is clearly favoured and the position of its maximum is also fairly constant ≈ 1.6 fm over a wide range of energies. The

³ The odd looking energy 578 MeV is chosen here, because about at this energy the maximum of the experimental total cross section of the reaction $pp \rightarrow d\pi^+$ is reached, which can be used for fixing the $NN \leftrightarrow N\Delta$ transition potential strength [5, 12].

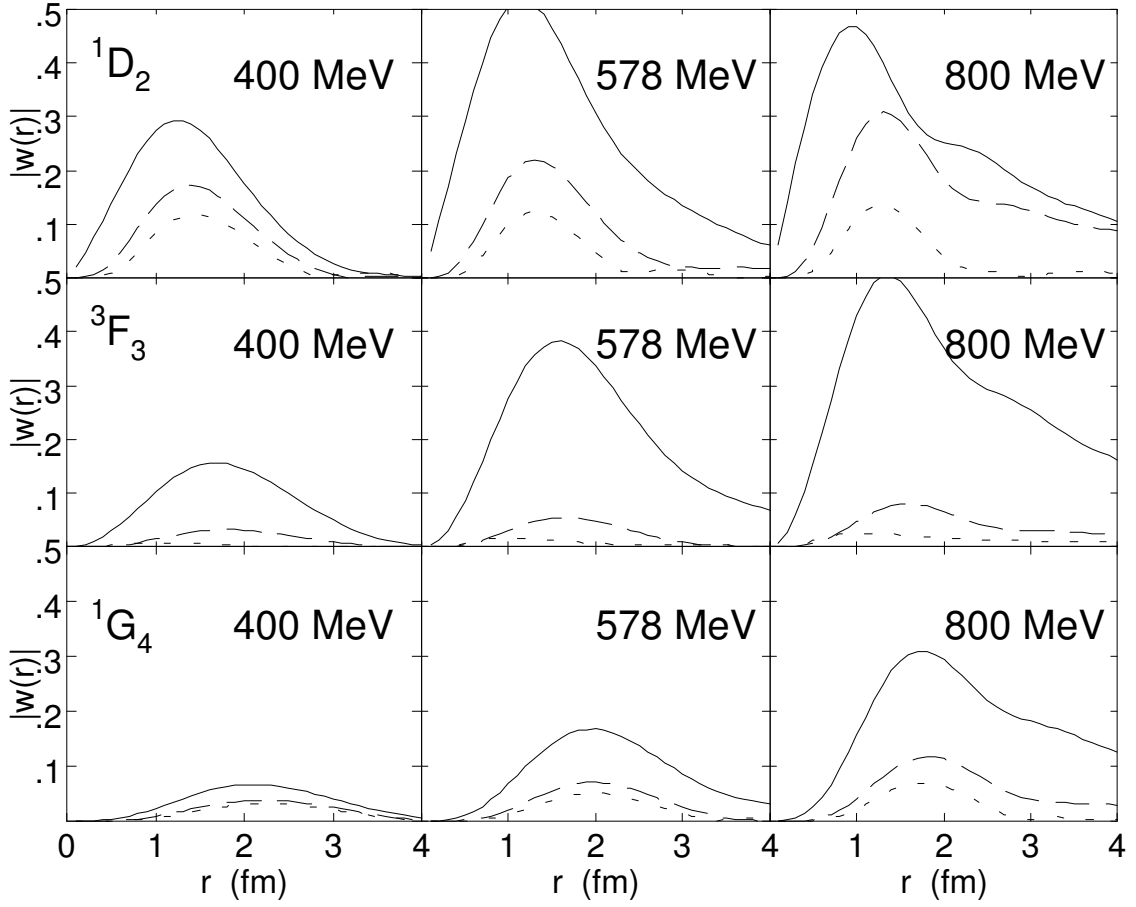


FIG. 1. Absolute values of the $N\Delta$ wave functions for the best “dibaryon” NN initial states at three laboratory energies. The curves are explained in the text.

dashed and dotted curves correspond to the much smaller ${}^5F_3(N\Delta)$ and ${}^3F_3(N\Delta)$ states, respectively. Remarkably, also in this case the effect of the $N\Delta$ angular momentum L' has only minuscule influence on the position of the maximum, whereas in comparison to the above ${}^1D_2(NN)$ case the *initial* NN wave being different with $L = 3$ has a larger effect. Again at highest energies the position of the maximum tends towards smaller distances, a behavior to be discussed later. It is also worth noting that in the case of ${}^3F_3(N\Delta)$ the tensor and spin-spin like parts of the transition potential act mutually destructively making the ${}^3F_3(N\Delta)$ wave negligible. The high ${}^5H_3(N\Delta)$ component is not included.

A third possible candidate satisfying the “dibaryon” conditions discussed in the previous sections has already quite a high angular momentum ${}^1G_4(NN)$. The preferred $N\Delta$ angular momentum state is now ${}^5D_4(N\Delta)$, about as distinct as the previous ${}^5D_2(N\Delta)$ as seen in

the lowest L series of Fig. 1 (solid curve). The ${}^5G_4(N\Delta)$ and ${}^5I_3(N\Delta)$ waves (dashed and dotted curves) are smaller but not negligible. Again the position of the maximum depends on the energy and L' only rather weakly, whereas the initial $L = 4$ of the initial nucleons has pushed the maxima to about 2 fm. The ${}^5D_4(N\Delta)$ maximum levels to ≈ 0.37 around 1100 and 1200 MeV. So the possible peaking of the energy distribution would be rather wide in this region.

A common systematic feature in the different states is that with increasing energy, above 600 MeV, there is a common (albeit weak) tendency for the maximum to creep towards smaller distances, since then also the incident particles get closer to each other through their centrifugal barrier. Another is that one may well speculate of some effective threshold, appearing as a cusp peak which in the case of ${}^1D_2(NN)$ is passed around 600 MeV (in ${}^5S_2(N\Delta)$ and may be reached for ${}^3F_3(NN)$ at about 800 MeV (in ${}^5P_3(N\Delta)$), whereas for ${}^1G_4(NN)$ it is still ahead. This expectation is confirmed by actual calculations as noted above. It is also worth noting that the formally calculated widths [17] are about 100 MeV at the relevant energies of maximal wave functions in full agreement with Yokosawa [22].

Now it may be of interest to have a look at states which do *not* satisfy the optimal conditions for “dibaryons” discussed earlier. The first such study may well come from the lowest L state, ${}^1S_0(NN) + {}^5D_0(N\Delta)$, shown on the first row of Fig. 2. The magnitude of the wave function is quite considerable, though it remains practically independent of energy. So it is not likely to produce such energy dependent behavior as resonances. In fact, the inclusion of the ${}^5D_0(N\Delta)$ component into the wave function introduces very strong attraction – even tens of degrees into the phase shift δ_0 . At the lowest energy 400 MeV the maximum is just at 1 fm and with increasing energy creeps to a slightly closer radius, to about 0.8 fm at 800 MeV. With its magnitude it looks quite strange that this state contributes very little to the reaction $pp \rightarrow d\pi^+$. A partial reason is that the NN and $N\Delta$ contributions tend to cancel rather completely in the 1S_0 amplitude to this reaction. Also, in overlap integrals this $N\Delta$ component mainly requires the smaller D -wave component of the deuteron.

The ${}^3P_1(NN)$ wave has three $N\Delta$ mixing states ${}^5P_1(N\Delta)$, ${}^5F_1(N\Delta)$ and ${}^3P_1(N\Delta)$ shown next in Fig. 2 by solid, dashed and dotted curves, respectively. In this case there is a strong energy dependence in the P -wave $N\Delta$ components with ${}^5P_1(N\Delta)$ reaching 0.6 at 800 MeV. The maximum (in r variable) levels to this value at 900 MeV and turns then slowly down,

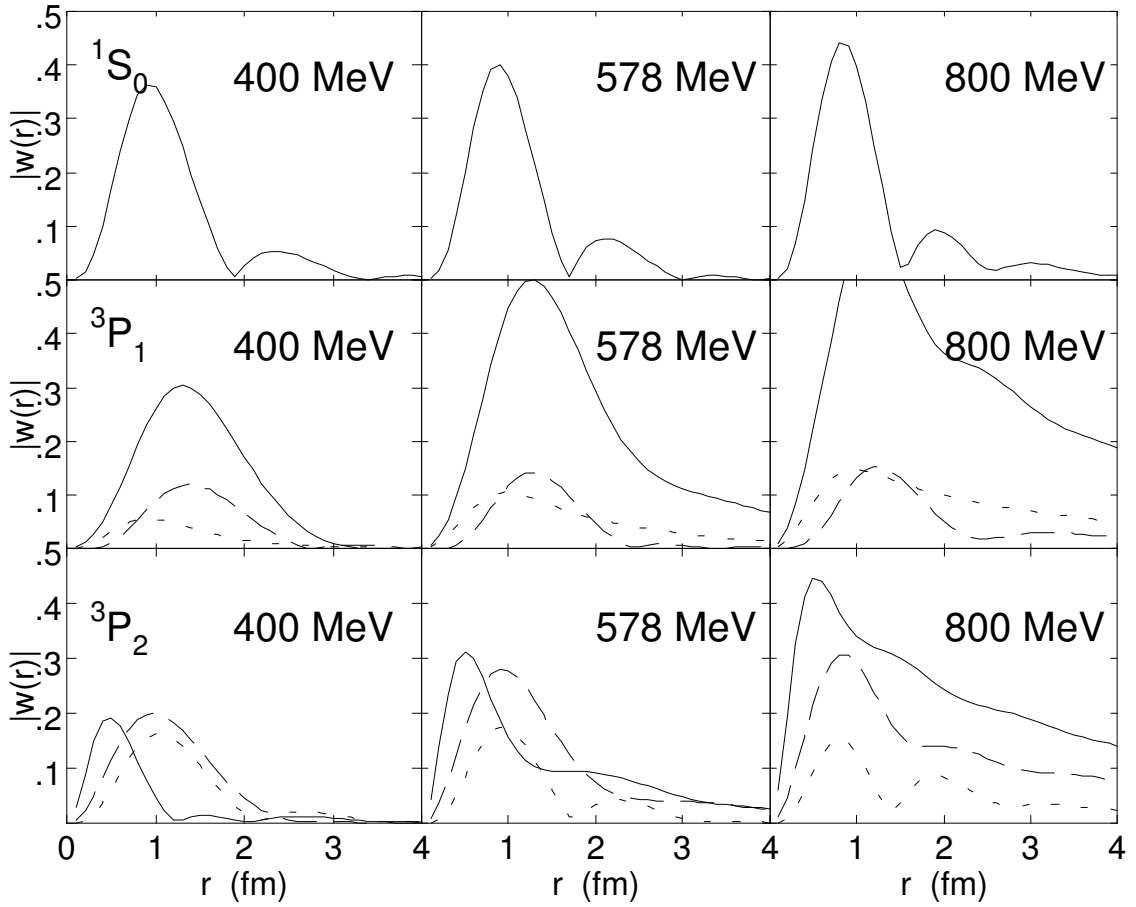


FIG. 2. Absolute values of the $N\Delta$ wave functions for the “bad” dibaryon NN initial states. The curves are explained in the text.

so slowly that the r -maximum remains within 2% from this value from 800 to 1000 MeV. One might imagine a resonance at this energy, but the background 3P_1 phase shift is going down so fast with increasing energy that perhaps it is not possible to see any “dibaryon” in this wave, in particular since the energy dependence of the very wide peak may be too slow. In the reaction $pp \rightarrow d\pi^+$ this wave gives rise to s -wave pions and pion-nucleon s -wave rescattering interferes destructively so that basically the corresponding amplitude is quite flat and very small rather soon above threshold, say above 400 MeV [6]. The dotted curve, ${}^3P_1(N\Delta)$, deviates slightly from the behavior of others, since it has also a moderate contribution from the spin-spin type transition potential [6], whereas the others arise purely from the tensor type. This coupling stresses typically shorter ranges.

The $N\Delta$ components in the tensor coupled ${}^3P_2 - {}^3F_2$ NN initial states are somewhat

smaller. The lowest row of Fig. 2 shows those arising from the state with the initial asymptotic wave ${}^3P_2(NN)$ boundary condition, although by the earlier arguments initial ${}^3F_2(NN)$ might be presumed to be dominant. The solid curve shows the ${}^3P_2(N\Delta)$ component and the dashed one ${}^5P_2(N\Delta)$. The former now arises dominantly from the spin-spin coupling, which clearly tends to emphasize smaller ranges than the tensor. In spite of its formally two times stronger transition potential [6] the ${}^5F_2(N\Delta)$ (dotted) is clearly smaller than the P -waves and the ${}^3F_2(N\Delta)$ (not shown) again roughly one half of this. The minima reflect the nodes of the initial partial wave. Lacking these nodes at small distances, the $N\Delta$ admixtures in ${}^3F_2(NN)$ are smoother but also smaller than in ${}^3P_2(NN)$, about half of these in height with their maxima ≈ 0.2 situated at 1.5 fm again showing the effect of the initial L to the $N\Delta$ wave function.

B. Phase considerations

In some approaches to $N\Delta$ effects (e.g. [31] and [32] for pion production) the mixing wave functions are considered more or less implicitly in a factorization approximation $w(r) \approx V_2(r)u(r)/(E - \Delta + i\Gamma/2)$. Therefore, it may also be of interest to compare this approach by plotting the phase of the coupled wave function relative to the NN wave function. Namely, since differential observables, in particular polarization phenomena, are sensitive to the phases of the amplitudes, also this phase may matter in reactions where $N\Delta$ components are active participants. Further, it should be noted that the L' dependence of the width, generated by the wave function structure [12, 17], is not often included.

This kind of treatment may give the total cross section peaking by construction relatively trivially [31]. However, as shown e.g. in Ref. [33], due to the different centrifugal barriers even the relative sizes of the $N\Delta$ components ${}^5S_2 + {}^5D_2 + {}^5G_2$ coupled to ${}^1D_2(NN)$ would come wrong as pointed out also in Subsec. III A. This kind of effects and also phase interferences lead to incorrect differential cross sections [34, 35] and spin observables [36] in $pp \leftrightarrow d\pi^+$. Differential observables are not tested at all in e.g. the “hidden dibaryon” approach to $pp \rightarrow d\pi^+$ of Ref. [32]. It is doubtful that this test would be passed.

Clearly, in this approximation division of $w(r)$ by $u(r)$ should rid the wave function from the overall nucleonic phase shift $e^{i\delta}$ so that the resulting function should only have a phase from the propagator, independent of r , and from the sign of $V_2(r)$. Fig. 3 for ${}^5S_2(N\Delta)$ and

${}^5D_2(N\Delta)$ admixtures in the ${}^1D_2(NN)$ state at 578 MeV shows this simple assumption to be problematic. This energy is chosen very close to the threshold cusp to maximize the presence of the resonant cusp effect. Obviously zero and 180 degree phases (modulo 360 degrees) would correspond to the same or opposite signs between the wave functions, which, in turn, is connected to the sign of the transition potential $V_2(r)$. Below and close to pionic threshold, naturally, this remaining relative phase alternates between $\pm 180^\circ$ and 0. In the presence of strong inelasticity this behavior is more blurred and Fig. 3 should be understood analogously in terms of the complex wave function “changing signs”. So in Fig. 3 the solid curve below 2 fm corresponds to positive $V_2(r)$ and positive *vs.* negative NN and $N\Delta$ wave functions, and oppositely the dashed curve to negative $V_2(r)$ and positive NN and $N\Delta$ wave functions, until, at 2 fm, the NN wave function changes sign (or more literally $e^{-i\delta}u(r)$ changes sign; with stronger inelasticity even this would have significant imaginary component in addition to the one generated in $N\Delta$). Of course, in actual amplitudes r -dependence is integrated over.

The phase from the propagator $(E - \Delta - i\Gamma/2)^{-1}$ can be easily compared. In the comparison one should also be aware that, as stated previously, the width is state dependent [17]. The straight horizontal lines show the phases arising from the propagator of the factorization with three different widths. First, the thick line presents the result without state dependence calculated as in Ref. [31] associated with $pp \rightarrow d\pi^+$ using the width

$$\Gamma = \frac{2}{3} \frac{f^{*2}}{4\pi} \frac{q^3}{\mu^2} \quad (5)$$

with μ and q the pion mass and momentum. Ref. [31] adopted $f^* = 2f$ from Chew-Low theory and the πNN coupling $f^2/4\pi = 0.08$ giving $\Gamma = 114$ MeV at this energy. For the Δ mass the real part of the position of the pole 20 MeV below the nominal Δ mass is used in the present calculations. The normal solid line, actually indistinguishable from the thick one, is the result using the ${}^5S_2(N\Delta)$ width 78 MeV from Ref. [17]. Because in the proximity of the Δ threshold the widths are much larger than $|E - \Delta|$, the thick and normal solid lines are both very close to 90 degrees. Further from the $\Delta - N$ mass difference the lines would be distinguishable. The dashed line has a much smaller width 11.5 MeV for ${}^5D_2(N\Delta)$ and also the negative sign of $V_2(r)$ is included.

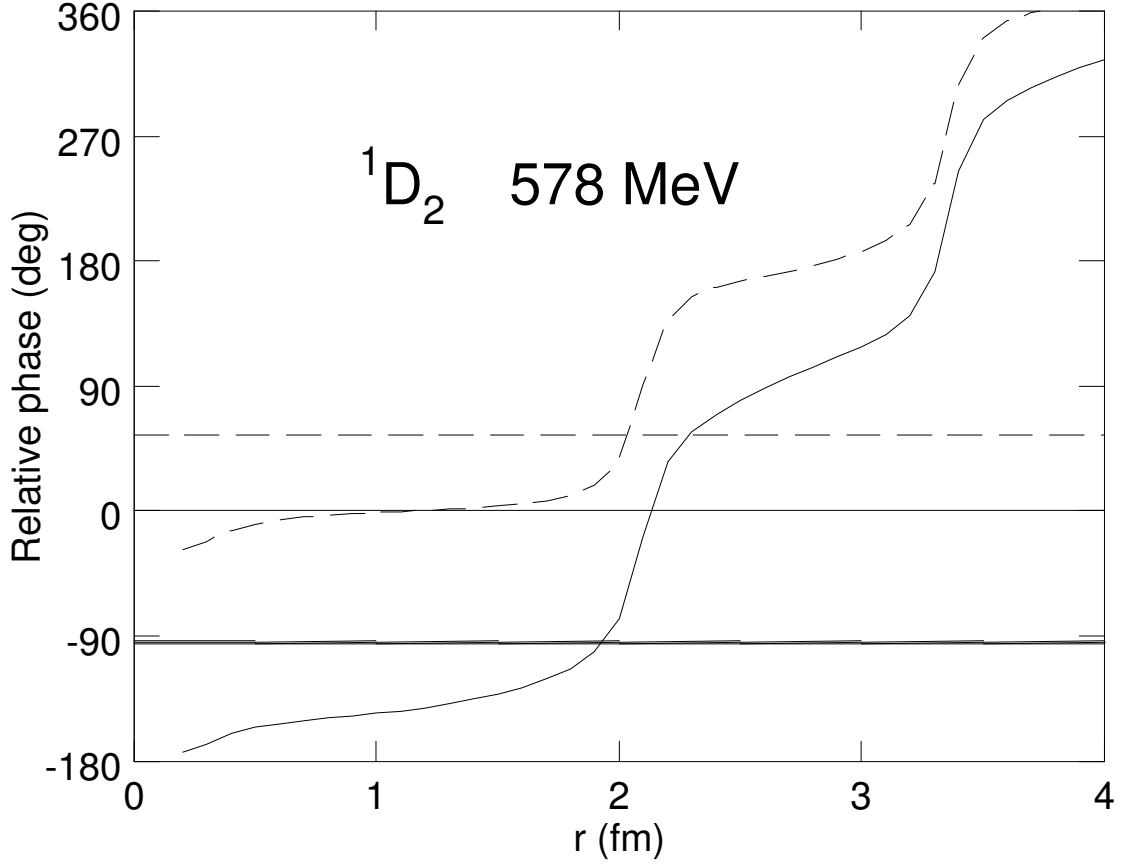


FIG. 3. Relative phase between $N\Delta$ and NN wave functions for the best dibaryon NN initial state 1D_2 at 578 MeV laboratory energy. The solid and dashed curves present $^5S_2(N\Delta)$ and $^5D_2(N\Delta)$, respectively. The horizontal lines show the phase of the $N\Delta$ propagator, independent of r , as explained in the text.

C. Effective thresholds

Finally, the expectation values of the centrifugal barrier $\hbar^2/(2m'r^2)$ are calculated for the three energies discussed and several $N\Delta$ states. From the results shown in Figs. 1 and 2, apart from the factor $L'(L' + 1)$, one would anticipate these to be rather similar within each NN state. One can deduce the average centrifugal energies in each state explicitly as presented in Table I, to be added to the mass difference $\Delta - M$ to get an effective threshold. And really, for the $N\Delta$'s coupled to $^1D_2(NN)$ at 578 MeV the expectation value $\langle 1/r^2 \rangle$ is 0.67 fm^{-2} for $^5D_2(N\Delta)$, while for $^5G_2(N\Delta)$ it is 0.68 fm^{-2} , the same within 2%. (The

TABLE I. Expectation values of centrifugal (left columns) and internal radial kinetic energies (right columns) for three intermediate NN laboratory energies in $N\Delta$ states (MeV). These should be added to the $N\Delta$ mass to get the corresponding effective threshold masses.

NN	$N\Delta$	400 MeV		578 MeV		800 MeV	
1D_2	5S_2	0	44	0	45	0	88
	5D_2	133	192	147	209	112	186
	5G_2	398	457	484	578	499	616
3F_3	5P_3	33	67	36	68	39	113
	5F_3	157	198	189	237	165	222
1G_4	5D_4	59	89	65	94	64	131
	5G_4	173	207	214	257	214	264
1S_0	5D_1	298	438	331	509	365	580
3P_1	5P_1	53	111	52	100	47	133
	3P_1	100	178	77	100	59	147
	5F_1	262	340	308	408	288	382
3F_2	5P_2	38	72	36	66	33	110
	3P_2	50	76	43	70	41	113
	5F_2	172	212	188	234	151	212
	3F_2	124	177	151	215	146	214
3P_2	5P_2	102	184	104	181	92	206
	3P_2	430	561	293	388	147	249
	5F_2	484	532	595	686	548	686
	3F_2	425	509	518	657	589	791

reduced mass to give $\hbar^2/(2m') = 36.54 \text{ MeVfm}^2$ has been used.)

However, there is a slight but larger dependence on energy as can be seen following the horizontal rows, but this is not particularly systematic. The most systematic dependence of the centrifugal energy (apart from the factor $L'(L' + 1)$) is on the angular momentum L of the initial NN state calculated for a fixed $N\Delta$ angular momentum L' : the larger L , the smaller E_{cent} . This resembles the trend quoted earlier and seen in Ref. [20]: decrease of the orbital angular momentum in the transition $NN \rightarrow N\Delta$ is favoured. The effective

threshold is then clearly lower than for $L' \geq L$. One can perhaps recognize the likeness of the behavior with a soft rotator: the larger angular momentum stretches the rotator increasing its moment of inertia and decreasing the related energy quanta. However, here the “stretching” angular momentum is mainly associated with the external NN state, not the internal $N\Delta$. For higher angular momenta the incident nucleons remain further and the transition is more peripheral leading also to a larger average distance between the nucleon and the Δ . In contrast, within the $N\Delta$ configuration the short-range r^{-2} repulsion is also counteracted by a higher barrier at larger distances deepening the classically forbidden region and damping the tunneling into asymptotic ranges. The r^{-2} dependence has longer range than the strong interaction or the extent of the confined wave function. The situation may be compared with e.g. hydrogen atom states, where the electron probability density is not strongly pushed to asymptotic regions by the centrifugal barrier - only rather the short-range behavior is affected. So e.g. in the ${}^5D_4(N\Delta)$ state (coupled to ${}^1G_4(NN)$) the above expectation value $\langle 1/r^2 \rangle$ is 0.27 fm^{-2} , while in the ${}^5G_4(N\Delta)$ it is nearly the same 0.24 fm^{-2} but nevertheless $\approx 10\%$ smaller. However, in comparison with the ${}^1D_2(NN)$ initial state the difference is towards even qualitatively smaller centrifugal energies, i.e. towards larger r^2 , with a factor of ≈ 2 between the two.

The expectation value of the kinetic energy associated with the radial degree of freedom also increases with angular momentum L' but most strongly with energy above the nominal $N\Delta$ threshold. However, below, say $E(\text{lab}) \approx 600 \text{ MeV}$, this is relatively constant and, added together with the centrifugal energy to the $N\Delta$ mass difference, might be considered to imply some kind of an effective threshold. Its nearly linear dependence above the nominal threshold apparently means that much of the excess NN energy can be seen to emerge in this way within the $N\Delta$ system. The increasing kinetic energy means more curvature of the wave function and the nodes (and maxima) coming closer to zero as was seen in Figs. 1 and 2 after 600 MeV.

Fig. 4 represents the effective thresholds thus calculated for the lowest energy $N\Delta$ admixture components, shown in Table I, as functions of the total center-of-mass energy \sqrt{s} . The lowest, solid line would be the lightest one, ${}^5S_2(N\Delta)$, associated with the ${}^1D_2(NN)$ initial state. Compared with the lowest energy dibaryon suggested by Yokosawa [22] (hollow square) this threshold would need some 20–40 MeV attraction. However, this requirement would conform very well with the early estimates for the $N\Delta$ binding energy of Arenhövel

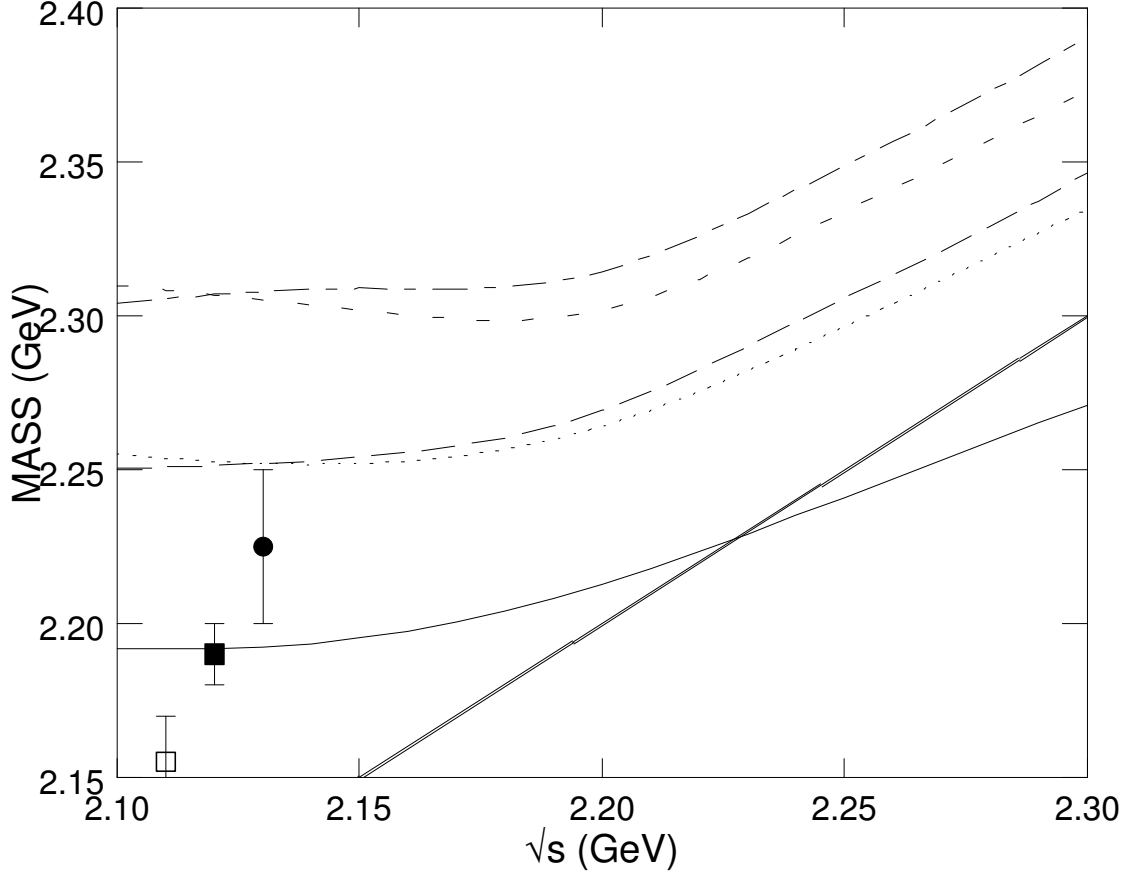


FIG. 4. The $N\Delta$ mass combined with the expectation value of the kinetic energy components (centrifugal and radial) for 5S_2 (solid), 5P_3 (long dashes), 5D_4 (dash-dot), 5P_2 from ${}^3F_2(NN)$ (dotted) and 5P_1 (short dashes). The thick line shows the total energy \sqrt{s} also on the mass scale. The points indicate three dibaryon masses suggested in Ref. [22].

[37] (actually calculated for isospin 2 to avoid coupling to the always open NN decay channels with isospin 1). A downward shift of the $N\Delta$ peak by about 20 MeV is also found in photodisintegration of deuterons in Ref. [38], if pion exchange interaction is added between the nucleon and the Δ . Therefore, $N\Delta$ attraction might allow the solid line to be accommodated with the mass range 2.14–2.17 MeV. The long dashes present the threshold of the ${}^5P_3(N\Delta)$ component arising from ${}^3F_3(NN)$. This is quite well established and the shoulder in its NN phase shift is very well described by the isobar coupling [17]. Also its important role in the successful description of polarization phenomena as well as differential cross section in $pp \rightarrow d\pi^+$ was first stressed in Ref. [6]. Now, its energy conforms rather well with

the suggestion of Yokosawa as the possible 3F_3 dibaryon resonance at 2.20–2.25 MeV [22] (filled circle). Both of these points also agree well with Hoshizaki’s ${}^1D_2(2.17)$ and ${}^3F_3(2.22)$ diproton resonances [39, 40]. The filled square indicates also Yokosawa’s suggestion for a further possible triplet P dibaryon (with a question mark) at 2.18–2.20 MeV. For this kind of low threshold the present calculation would indicate rather as the starting NN state 3F_2 (dotted curve) but still significantly higher than Ref. [22] (by ≈ 60 MeV). The 3P_1 initial state (short dashes), in turn, would yield still about 50 MeV more overestimate and 3P_2 still much more as seen from Table I.

Also indicated by the thick line in Fig. 4 is the c.m. energy itself on the mass axis. Namely for a resonance this line should cross the threshold or resonance mass curve. This does happen for the ${}^5S_2(N\Delta)$ case, actually at the same energy as the calculated ${}^1D_2(NN)$ Argand diagram line crosses the y-axis in Fig. 5 of Ref. [17]. Therefore, in this respect the ${}^5S_2(N\Delta)$ threshold effect resembles a true resonance. However, in other cases the excess energy above threshold in the $N\Delta$ states causes the crossing point to escape. Consequently, the Argand diagram of the ${}^3F_3(NN)$ “dibaryon” stays on the left side of the y-axis in that figure, although the corresponding shoulder of the phase shift in Fig. 6 (Ref. [17]) mimics well a resonance. Both diagrams have exactly the same behavior as found in energy-dependent and energy-independent phase shift analyses by Arndt *et al.* [41].

There are two higher energy dibaryon suggestions by Yokosawa, both at 2.43–2.50 GeV (1G_4 and a triplet state). The dash-dot curve shows the described calculation for the former as too low by over a hundred MeV as well as a candidate ${}^3P_1(NN)$ also for the latter one (short dashes). However, due to the energy dependence of the calculated expectation values the low-end threshold results may not be totally relevant in the case of higher energies where the effective threshold is also larger and rapidly increasing.

Though it seems from Fig. 4 that in the ${}^5D_4(N\Delta)$ state the threshold cannot be reached and crossed, it may still be of some interest to study the behavior of the wave functions more directly for qualitative insights. In the context of Figs. 1 and 2 it was seen that the maxima of the wave functions for $L' > 0$ could still continue growing beyond 800 MeV laboratory energy (beyond 2.25 GeV mass). So even if this crossing does not take place, there might appear some wide resonance-like peaking. Fig. 5 shows this $N\Delta$ wave function at $r = 1.5$ fm as an Argand diagram arrangement (circles). At this distance the absolute value of the wave function at 1100 MeV energy has its maximum. This is also the energy at which the

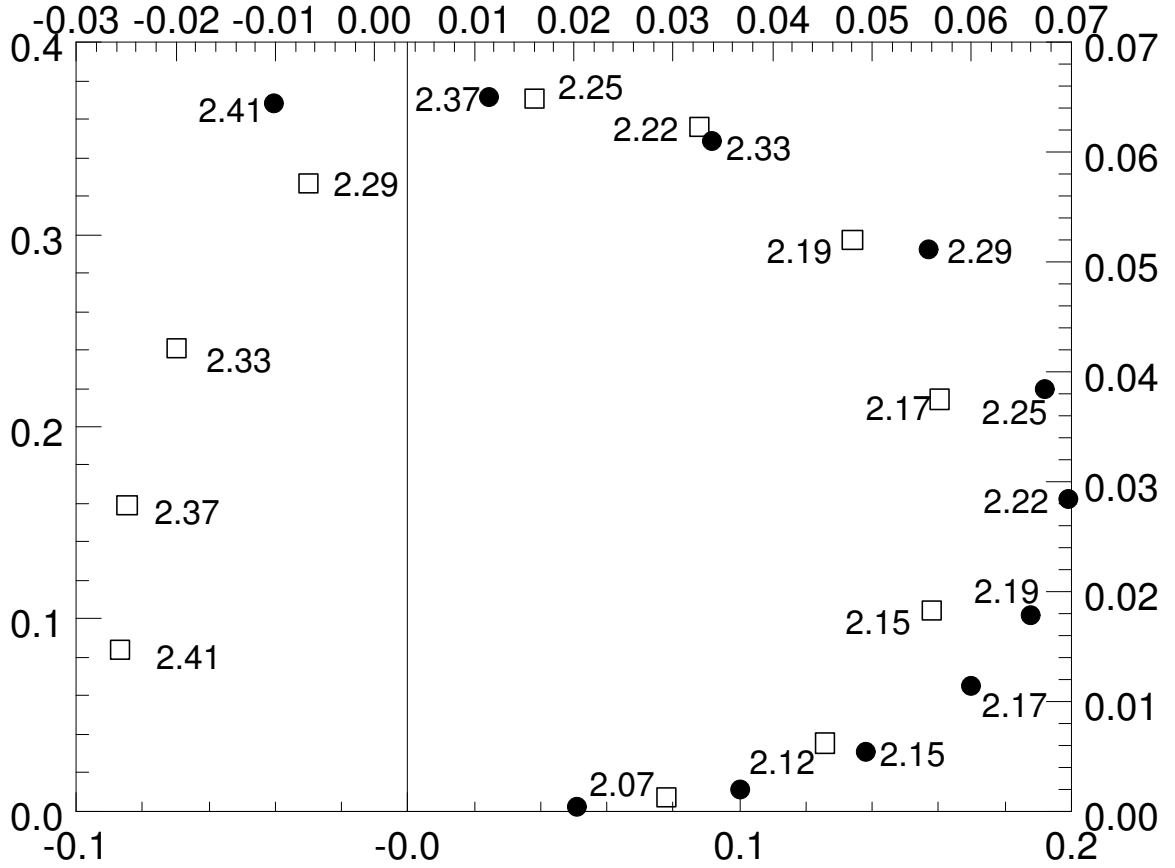


FIG. 5. Circles: ${}^5D_4(N\Delta)$ wave function at 1.5 fm for different c.m. energies (in GeV) imitating an Argand plot (left and bottom scale). The overlap integral discussed in the text (in $\text{fm}^{1/2}$) shown by squares in top and right scale. The imaginary axis (real part zero point) is given for the former. Unessential overall minus sign is omitted.

peak (outside Fig. 1) levels to a very wide global maximum ≈ 0.37 . The idea is that the weighted wave function at some optimized distance would be qualitatively representative for the behavior of the corresponding amplitude. The archetypal circle is featured, which crosses the imaginary axis (drawn for this quantity) approximately for 2.39 GeV. So, even though the c.m. energy does not formally reach the escaping effective threshold (2.45 GeV at this incident energy) from Fig. 4, the corresponding amplitude can still have some resonance-like behavior reasonably close to Yokosawa's experimental suggestion 2.43 MeV. Further, shown

by the squares is the overlap integral

$$I(^5D_4(N\Delta)) = \int_0^\infty w_D(r) j_0(qr/2) w_{N\Delta}(r) dr \quad (6)$$

appearing in f -wave pion production in reaction $pp \rightarrow d\pi^+$ (here $w_D(r)$ is the D -wave component of the deuteron and q the center-of-mass momentum of the pion). A similar resonance circle emerges. However, the spherical Bessel function stresses the shorter ranges and so this overlap crosses the imaginary axis at a lower energy than the representative fixed-point value of the wave function.

IV. CONCLUSION

In this work the effect of the centrifugal barrier in the $N\Delta$ configurations coupled to initial NN states has been considered from different angles. First the effect on the magnitude of the wave function as a function of r is studied for different angular momentum situations. It was seen that, contrary to the first expectation, the angular momentum L' of the $N\Delta$ system itself has very little effect on the shape of the wave function, only on the overall magnitude with higher repulsions decreasing the probability of high L' $N\Delta$ admixtures. This agrees with the finding of a more phenomenological calculation [20]. However, the initial NN angular momentum L has a more significant influence in pushing the $N\Delta$ system apart.

Next the association of the state dependent width as a uniform imaginary potential with the phase of the $N\Delta$ admixture is studied comparing the coupled channels results with simpler models of separable wave functions. Significant differences are seen especially considering that normally such models do not include angular momentum dependence of the width implied in self-consistent coupled channels calculations [17].

It is also suggested that, due to the fact that in the complex potential now the $N\Delta$ wave function is confined producing finite expectation values for the centrifugal barrier and kinetic energy, it is possible to define effective thresholds higher than the nominal mass barrier $M_\Delta - M_N$ for different $N\Delta$ components. This explains some parts of the wave function behavior seen above. Due to kinetic energy being assimilated in the configurations, these thresholds have strong energy dependence above the nominal mass difference. In spite of the thresholds escaping higher and higher with increasing energy it was possible to see some resemblance to resonant behavior in the $N\Delta$ wave functions and the transition amplitudes

as exemplified in Fig. 5 for the ${}^5D_4(N\Delta)$ component originating from ${}^1G_4(NN)$. It may be noted that these results can be regarded as kinematic consequences. Any strong interaction model between the nucleon and the Δ is not attempted here.

Apart from slight deviations these findings are qualitatively in line with those of Ref. [20]. The difference of principle is that in Ref. [20] the phase equivalence was forced to the interaction with and without the $N\Delta$ coupling, while here no such constraint is explicitly imposed though the phase shifts of e.g. Arndt *et al.* [41] are well reproduced. Of course, that constraint implicitly incorporates also the finite kinetic energy of the $N\Delta$ system. To counteract the strongly attractive $N\Delta$ box and its iterations by repulsive $[V_2(r)]^2/\Delta E$ the denominator ΔE needs to become even smaller than $\Delta - N$ mass difference (in the absence of the centrifugal barrier in ${}^5S_2(N\Delta)$ state). By definition, this is not possible in the present work. Similar systematics holds also for the triplet states. In general, this energy denominator remains thus somewhat smaller than the presently calculated effective thresholds. Numerically, apparently the implicit combination of the centrifugal energy and the L' dependent radial kinetic energy gave larger quanta of 40 MeV attributed to the centrifugal part in Ref. [20] as the overall rotational series $\text{const} + 40L'(L' + 1)$ MeV. A quick look at Table I confirms this simplified prescription as well valid for the 1D_2 and 3P_1 NN states, but only qualitatively elsewhere with smaller energy quanta ≈ 30 MeV.

Numerically the effective thresholds for the lowest L' $N\Delta$ states shown in Table I and Fig. 4 agree relatively well with the suggested isospin one 1D_2 and 3F_3 dibaryons. Also the state 1G_4 can get some qualitative illumination in terms of $N\Delta$ wave functions. Moreover the widths are agreeable at relevant masses as shown earlier e.g. in Ref. [17].

-
- [1] A. M. Green, Rep. Prog. Phys **39**, 1109 (1976).
 - [2] H. J. Weber and H. Arenhövel, Phys. Rep. **36**, 277 (1978).
 - [3] C. Hanhart, Phys. Rep. **397**, 155 (2004).
 - [4] J. Hoftiezer *et al.*, Phys. Lett. B **100**, 462 (1981).
 - [5] J. Hoftiezer *et al.*, Nucl. Phys. A **402**, 429 (1983).
 - [6] J. A. Niskanen, Nucl. Phys. A **298**, 417 (1978).
 - [7] J. A. Niskanen, Phys. Lett. B **79**, 190 (1978).

- [8] J. A. Niskanen, Phys. Lett. B **82**, 187 (1979).
- [9] E. Aprile *et al.*, Nucl. Phys. A **379**, 369 (1982).
- [10] E. Aprile *et al.*, Nucl. Phys. A **415**, 365 (1984).
- [11] H. Kamo and W. Watari, Prog. Theor. Phys. **62**, 1035 (1979).
- [12] J. A. Niskanen, Phys. Lett. B **141**, 301 (1984).
- [13] A. M. Green and M. E. Sainio, J. Phys. G: Nucl. Phys. **8**, 1337 (1982).
- [14] W. Leidemann and H. Arenhövel, Nucl. Phys. A **465**, 573 (1987).
- [15] P. Adlarson *et al.*, Phys. Rev. Lett. **106**, 242302 (2011).
- [16] P. Adlarson *et al.*, Phys. Lett. B **721**, 229 (2013).
- [17] J. A. Niskanen, Phys. Rev. C **95** (2017) 054002; arXiv:1610.06013 [nucl-th].
- [18] A. Gal and H. Garcilazo, Phys. Rev. Lett. **111**, 172301 (2013).
- [19] A. Gal and H. Garcilazo, Nucl. Phys. A **928**, 73 (2014).
- [20] J. A. Niskanen, Phys. Lett. B **112**, 17 (1982).
- [21] R. Reid, Ann. Phys. **50**, 411 (1968).
- [22] A. Yokosawa, Phys. Rep. **64**, 47 (1980).
- [23] A. Yokosawa, proc. 6th Int. Symp. on Polarization. Phenomena in Nuclear Physics, Aug. 1985, Osaka, Japan, J. Phys. Soc. Jap. Suppl. **55** (1986); Report ANL-HEP-CP-85-93.
- [24] H. Sugawara and F. von Hippel, Phys. Rev. **172**, 1764 (1968).
- [25] M. Tanabashi *et al.* (Particle Data Group), Phys. Rev. **D 98**, 030001 (2018).
- [26] J. R. Taylor, *Scattering Theory*, (John Wiley, New York, 1972).
- [27] J. M. Blatt and L. C. Biedenharn, Rev. Mod. Phys. **24**, 258 (1952).
- [28] J. A. Niskanen, Phys. Rev. C **45**, 2648 (1992).
- [29] J. A. Niskanen, Phys. Rev. C **92**, 055205 (2015); arXiv:1502.03278 [nucl-th].
- [30] A. M. Green and J. A. Niskanen, Nucl. Phys. A **404**, 495 (1983).
- [31] M. Brack, D.-O. Riska and W. Weise, Nucl. Phys. A **287**, 425 (1977).
- [32] M. N. Platonova and V. I. Kukulin, Nucl. Phys. A **946**, 117 (2016).
- [33] J.A. Niskanen, Inv. talk at 5th Int. Symp. on Polarization Phenomena in Nuclear Physics, Santa Fe, Aug. 1980, AIP Conf. Proc. **69**, p. 62.
- [34] J. Chai and D.-O. Riska, Nucl. Phys. A **338**, 329 (1980).
- [35] O. Maxwell, W. Weise, and M. Brack, Nucl. Phys. A **348**, 388 (1980).
- [36] O. Maxwell and W. Weise, Nucl. Phys. A **348**, 429 (1980).

- [37] H. Arenhövel, Nucl. Phys. A **247**, 473 (1975).
- [38] J. A. Niskanen and P. Wilhelm, Phys. Lett. B **359**, 295 (1995).
- [39] N. Hoshizaki, Prog. Theor. Phys. **60**, 1796 (1978).
- [40] N. Hoshizaki, Prog. Theor. Phys. **61**, 129 (1979).
- [41] R. A. Arndt, L. D. Roper, R. A. Bryan, R. B. Clark, B. J. VerWest, and P. Signell, Phys. Rev. D **28**, 97 (1983).